THE JOURNAL OF BIOLOGICAL CHEMISTRY VOL. 286, NO. 10, pp. 8620–8632, March 11, 2011

Nuclear/Nucleolar GTPase 2 Proteins as a Subfamily of YlqF/YawG GTPases Function in Pre-60S Ribosomal Subunit Maturation of Mono- and Dicotyledonous Plants*[S]

Received for publication, November 5, 2010, and in revised form, December 28, 2010 Published, JBC Papers in Press, January 4, 2011, DOI 10.1074/jbc.M110.200816

Chak Han Im[‡1], Sung Min Hwang[‡2], Young Sim Son[‡1], Jae Bok Heo[‡], Woo Young Bang[‡], I. Nengah Suwastika[§], Takashi Shiina[¶], and Jeong Dong Bahk[‡3]

From the [‡]Division of Applied Life Sciences (BK21), Graduate School of Gyeongsang National University, Jinju 660-701, Korea, the [§]Graduate School of Biostudies, Kyoto University, Sakyo-ku, Kyoto 606-8502, Japan, and the [¶]Graduate School of Human and Environmental Sciences, Kyoto Prefectural University, Shimogamo, Sakyo-ku, Kyoto 606-8522, Japan

The YlqF/YawG families are important GTPases involved in ribosome biogenesis, cell proliferation, or cell growth, however, no plant homologs have yet to be characterized. Here we isolated rice (*Oryza sativa*) and *Arabidopsis* nuclear/nucleolar GTPase 2 (OsNug2 and AtNug2, respectively) that belong to the YawG subfamily and characterized them for pre-60S ribosomal subunit maturation. They showed typical intrinsic YlqF/YawG family GTPase activities in bacteria and yeasts with k_{cat} values 0.12 ± 0.007 min^{-1} ($n = 6$) and 0.087 ± 0.002 min^{-1} ($n = 4$), respectively, and addition of 60S ribosomal subunits stimulated their activities *in vitro*. In addition, OsNug2 rescued the lethality of the yeast *nug2* null mutant through recovery of 25S pre-rRNA processing. By yeast two-hybrid screening five clones, including a putative one of 60S ribosomal proteins, OsL10a, were isolated. Subcellular localization and pulldown assays resulted in that the N-terminal region of OsNug2 is sufficient for nucleolar/nuclear targeting and association with OsL10a. OsNug2 is physically associated with pre-60S ribosomal complexes highly enriched in the 25S, 5.8S, and 5S rRNA, and its interaction was stimulated by exogenous GTP. Furthermore, the *AtNug2* knockdown mutant constructed by the RNAi method showed defective growth on the medium containing cycloheximide. Expression pattern analysis revealed that the distribution of *AtNug2* mainly in the meristematic region underlies its potential role in active plant growth. Finally, it is concluded that Nug2/Nog2p GTPase from mono- and didicotyledonous plants is linked to the pre-60S ribosome complex and actively processed 27S into 25S during the ribosomal large subunit maturation process, *i.e.* prior to export to the cytoplasm.

In eukaryotes, ribosome biogenesis is a complex and coordinated process that involves the synthesis and processing of rRNA, and its assembly with ribosomal proteins (1, 2). Ribosome biogenesis begins with transcription of rDNA repeats by RNA polymerase I and III, followed by processing and assembly of pre-rRNA intermediates, which are exported to the cytoplasm from the nucleolus and nucleus (3–9). These processes require various ribosome biogenesis factors such as assembly factors, as well as non-ribosomal factors including snoRNPs, endo- and exonucleases, pseudouridine synthases, methyltransferases, RNA helicases, RNA chaperones, ATPases and GTPases (3, 4, 6–8, 10).

Several GTPases are essential for the biogenesis and assembly of ribosomal subunits (1, 10–13). In *Escherichia coli*, the process of the 50S ribosomal subunit assembly requires Obg, EngA, and HflX (14–16), whereas *Bacillus subtilis* needs YphC and YsxC (17–19). Interestingly, most GTPases involved in ribosomal biogenesis belong to the YlqF/YawG family, which is characterized by a circularly permuted order of GTPase motifs within the GTP-binding domain (1, 11, 20). In *E. coli*, YjeQ binds to the 30S ribosomal subunit, whereas YloQ and YqeH show similar activities in *B. subtilis* (21–23). YlqF (RbgA) participates in late stage assembly of the 50S ribosomal subunit in *B. subtilis* (24, 25).

Circularly permuted GTPases are also well conserved in eukaryotes, and GTPases Nug1 and Nug2 were identified originally in *Saccharomyces cerevisiae* (26, 27). Nug1 is involved in the 60S ribosome export from the nucleus to the cytoplasm (26, 28) and Nug2 depletion leads to an increase in 27SBs and 7Ss intermediates in the major rRNA processing pathway, which indicates that it is required for late 60S maturation in the nucleus and nucleolus (26, 27). In *S. cerevisiae*, Lsg1 has been characterized as a cytoplasmic protein that is essential for biogenesis of the 60S ribosome and ribosomal release of nuclear export factor Nmd3p (29, 30). Thus, it seems likely that many of these GTPases facilitate ribosome biogenesis when recruited to the system.

Recent studies on ribosomal proteins and ribosomal assembly factors have indicated that the ribosome plays a regulatory role in plant development (31, 32). In *Arabidopsis*, mutation of genes encoding large ribosomal proteins L23 and L24, or small ribosomal proteins RPS14 and RPS16, led to abnormal development and pleiotropic phenotypes (33–36). Similarly, silencing of ribosomal *L3* genes in *Nicotiana tabacum* resulted in significant alterations in plant growth, development, and ribosome biogenesis (37). In *Arabidopsis*, *PIGGYBACK* genes

* This work was supported in part by grants from the BK21 program of the Ministry of Education and Science Technology of Korea.
[S] The on-line version of this article (available at http://www.jbc.org) contains supplemental Table S1 and Figs. S1 and S2.
[1] Graduate student supported by the BK21 program, Gyeongsang National University of Korea, Jinju, Korea.
[2] Postdoctoral student supported by the BK21 program, Gyeongsang National University of Korea.
[3] To whom correspondence should be addressed. Tel.: 82-55-751-6264; Fax: 82-55-759-9363; E-mail: jdbahk@gnu.ac.kr.

encoding 60S ribosomal proteins L10a, L9, and L5, specifically affect leaf patterning and development (38). Mutations in genes encoding important factors for plant 60S ribosome maturation, such as *AtNUC-L1*, *-L2,* and *PARL1*, caused similar morphological and developmental defects to those for 60S ribosomal proteins (39, 40).

Although several genes involved in ribosomal protein biogenesis have been identified in *Arabidopsis* and rice (supplemental Table S1), few have been characterized. Like yeast and mammals, plants may also contain modules for ribosome biogenesis. YawG subfamily proteins represent important candidates for this process; however, despite increasing knowledge regarding the functional roles played by these proteins, plant homologs remain to be characterized.

In this study, we report the identification and characterization of *OsNug2* and *AtNug2,* orthologs of yeast Nug2 essential for pre-60S ribosomal subunit maturation, in rice and *Arabidopsis*, respectively. These proteins exhibit intrinsic GTPase activity and OsNug2 can rescue a lethal yeast *nug2* null mutant. Through yeast two-hybrid screening of a rice cDNA library, OsL10a was identified as a putative 60S ribosomal protein. In particular, the GTP-bound form of OsNug2 shows increased affinity for the ribosome. A growth-defective phenotype of an *AtNug2* knock-down mutant grown on medium containing cycloheximide (CHX)[4] seems to be caused by lower translational efficiency resulting from a failure in pre-60S processing. Thus, this work reveals that both OsNug2 and AtNug2 function in the maturation process of the pre-60S ribosomal subunit in plants.

EXPERIMENTAL PROCEDURES

Sequence Alignment and Isolation of cDNAs Encoding Nug2 Genes in Rice and Arabidopsis— FASTA searches of the rice and *Arabidopsis* genomes were conducted using amino acid sequences from yeast YawG subfamily protein as a data base query. Sequence alignment of YawG subfamily proteins was performed using CLUSTAL W and BOXSHADE 3.21, for predictions with high homology sequences. *OsNug2* (Os03g22890) and *AtNug2* (At1g52980) cDNAs were prepared using reverse transcription (RT) and PCR. Primers were designed against nucleotide sequences deposited in the expressed sequence tag (EST) data base. PCR amplification was carried out as follows: 94 °C for 2 min, followed by 30 cycles of 94 °C for 30 s (denaturation), 52 °C for 30 s (annealing), 72 °C for 1 min 30 s (elongation), and then 72 °C for 5 min. Amplified DNA was separated by agarose gel electrophoresis and then bands were eluted and cloned into pGEM-T Easy (Promega).

Plant Materials and Generation of Transgenic Arabidopsis— For protoplast preparation, *Arabidopsis* was grown on agar plates containing MS/2 and 2% sucrose. RT-PCR analysis was performed on the japonica rice variety, Dongjin. Rice Oc cells were used for further experiments and prepared as described previously (41, 42). For construction of the *AtNug2* RNAi plasmid, a GUS fragment was used as a linker between *AtNug2* fragments in the antisense and sense orientations. The 500-bp *AtNug2* gene-specific region was produced by PCR amplification. This fragment was then cloned into the AscI-SwaI and BamHI-SpeI sites of pFGC1008. The resulting construct was introduced into *Agrobacterium tumefaciens* strain LBL4404 and the recombinant strain was then used to transform *Arabidopsis* ecotype Col-0 plants by the floral dip method. Transformants were subsequently selected on MS/2 medium containing 30 μg/ml of hygromycin and 100 μg/ml of cefotaxim. For *AtNug2* promoter-driven *GUS* expression, a 1,500-bp region upstream of *AtNug2* was amplified by PCR and then inserted into the pCAMBIA 1381 binary vector. Transformations and selection of *AtNug2* promoter:*GUS* constructs were performed in the same way as described for the *AtNug2* RNAi plasmid.

RT-PCR and Histochemical Staining—Total RNAs were isolated from various rice tissues using TRI-Reagent (Molecular Research Center), according to the manufacturer's instructions. Total RNA (1 μg) was used for RT-PCR analysis. cDNA was prepared using Moloney murine leukemia virus (MMLV) reverse transcriptase (Fermentas, Canada) and oligo(dT_{18}) primer, followed by amplification with specific primer pairs during 25 cycles of PCR.

Histochemical localization of GUS activity was performed as described by Jefferson *et al.* (43). In brief, wild-type or transgenic *Arabidopsis* seedlings, organs and tissues, were vacuum infiltrated in 50 mM KH_2PO_4 buffer (pH 7.2), 2 mM potassium ferrocyanide, 2 mM potassium ferricyanide, and 0.2% Triton X-100 containing 1 mM X-GlcA (Duchefa, Netherlands). Samples were incubated in the dark at 37 °C for 12 h and then transferred to 70% ethanol to remove chlorophylls. Digital images were obtained using an Olympus SZX12 stereoscope (Olympus, Japan).

GTP Hydrolysis Assay—GST-OsNug2 and GST-AtNug2 were expressed in *E. coli* BL21(DE3). Recombinant proteins were affinity purified using GST affinity columns containing glutathione-agarose 4B. Eluted proteins were further purified by gel-filtration chromatography (Superdex^{TM} 200 10/300 GL, Amersham Biosciences), followed by fast protein liquid chromatography (FPLC; Amersham Biosciences) and concentration with Centriprep (Millipore). GTP hydrolysis assays were performed on poly(ethyleneimine)-cellulose TLC plates with only a slight modification from the method described previously (44). In brief, reactions were performed in buffer containing 50 mM Tris-HCl (pH 8.0), 5 mM $MgCl_2$, 0.5 mM DTT, 1 mM EDTA, 1 mM NaN_3, 16.5 nM [α-^{32}P]GTP and each of the recombinant proteins at 30 °C. Aliquots (10 μl) were sampled at appropriate time intervals and reactions were stopped with an equal volume of 0.5 M EDTA (pH 8.0). Each sample (1 μl) was spotted onto a polyethyleneimine-cellulose TLC plate, which was then developed in 0.5 M NaH_2PO_4 (pH 3.4). After drying, the plate was exposed to a screen and signals were visualized using the Cyclone PhosphorImager (PerkinElmer Life Sciences). Finally, spots were quantified using OptiQuant software (Packard Instruments). To measure the turnover values (k_{cat}) of OsNug2 and AtNug2, reaction mixtures containing 3 μM GST-OsNug2 or GST-AtNug2 and 1 mM GTP in GTPase buffer (20 mM HEPES, pH 8.0, 1 mM $MgCl_2$, 0.5 mM DTT, and 1 mM NaN_3) were incubated at 30 °C for 15 h. The released phosphate was quantified with Biomol green regent (Biomol Research Labora-

[4] The abbreviations used are: CHX, cycloheximide; SC, synthetic complete; FW, fresh weight; GTPγS, guanosine 5′-3-*O*-(thio)triphosphate.

tories), according to the manufacturer's protocol. The catalytic constant was derived from $k_{cat} = \nu_{max}/c_{OsNug2}$.

UV Cross-linking—UV cross-linking reactions were performed as described previously (44). The purified GST-OsNug2 was incubated with 0.1 μM [α-^{32}P]GTP in 20 μl of reaction mixture (50 mM HEPES/KOH, pH 8.0, 1 mM $MgCl_2$, 1 mM EDTA, 50 mM KCl, 2 mM dithiothreitol, and 0.1% glycerol) for 15 min at 30 °C and 40 μM of competitors (*i.e.* ATP, CTP, GTP, GDP, and GMP) were added for 15 min at 30 °C. The mixture was irradiated on ice at a distance of 3 cm for 10 min using mineral light at a wavelength of 254 nm. After UV cross-linking, reactions were stopped by the addition of 5× SDS gel-loading buffer and separated by 10% SDS-PAGE. The gel was treated with 50 mM sodium phosphate buffer (pH 5.0) for 30 min at room temperature with a low-speed shaking, stained with Coomassie Blue, destained, dried, and exposed to a screen. Finally, the film was developed using the Cyclone PhosphorImager.

Complementation of Yeast Δnug2 Mutants—The heterozygous diploid yeast strain *S. cerevisiae* Y26080 (*MATa*/*MATα*, *his3Δ1*/*his3Δ1, leu2Δ0*/*leu2Δ0, lys2Δ0*/*LYS2, MET15*/*met15Δ0, ura3Δ0*/*ura3Δ0, YNR053c*::*kanMX4*/*YNR053c*) was purchased from Euroscarf (Frankfurt, Germany). The strain was transformed with recombinant pYES2 plasmid containing *OsNug2* cDNA under control of the *gal1* promoter. Haploid progeny were produced by plating on sporulation medium (1% KOAc, 1.25% yeast extract, 0.1% glucose, and 2% agar) for 5 days. After zymolyase digestion, the tetrads were dissected. Sporulated yeast cells bearing plasmids were selected on synthetic complete (SC) medium lacking uracil (SC-Ura) and viability was checked on SC medium lacking methionine and uracil (SC-MU) or lacking methionine, uracil, and lysine (SC-MUK). BY4743 (*MATa*/*MATα*, *his3Δ0*/*his3Δ0, leu2Δ0*/*leu2Δ0, met15Δ0*/*MET15, LYS2*/*lys2Δ0*; *ura3Δ0*/*ura3Δ0*) was used as a control.

Northern Blot Analysis and RNA Binding Assay—Total RNAs were isolated from yeast cells using the RNeasy Mini Kit system (Qiagen, Germany), according to the manufacturer's instructions. RNAs were separated by electrophoresis on 1.5% agarose-formaldehyde gels and transferred to Hybond nylon membranes (Amersham Biosciences). Membranes were probed with ^{32}P-labeled oligonucleotides complementary to specific regions, according to the manufacturer's instructions (Takara, Japan). Hybridization signals were visualized using a Cyclone PhosphorImager.

For the RNA binding assay, total cell lysates were obtained from Oc cells and incubated overnight with GST or GST-OsNug2 in reaction buffer (20 mM Tris-HCl, pH 8.0, 0.5 mM MgOAc, 0.2% Triton X-100, 150 mM KOAc, 1 mM DTT and protease inhibitors) at 4 °C. The reaction mixtures were incubated with glutathione-agarose 4B beads at 4 °C for 4 h and then the beads were washed three times with reaction buffer. Total RNAs were isolated from residual precipitates by adding phenol directly to the beads. Resuspended RNAs were separated by electrophoresis on 1.5% agarose-formaldehyde gels. Hybridization was performed as described above, using probes for specific rRNAs.

Yeast Two-hybrid Screening—LexA-based yeast two-hybrid screening was performed according to Hybrid Hunter instructions (Invitrogen). A rice cDNA library was constructed in pYEStrp2, which contains the B42-activation domain. The library was screened with yeast strain EGY48/pSH18-4. Yeast cells were cotransformed with bait plasmid encoding the LexA DNA-binding domain fused to OsNug2 (LexA-OsNug2) and 100 μg of library plasmid. Transformants were selected on synthetic complete (SC) medium lacking uracil, histidine, and tryptophan (SC-UHW). Colonies were replated onto synthetic complete medium lacking uracil, histidine, tryptophan, and leucine (SC-UHWL). Colonies that grew on selection medium after 2–4 days were picked and positive colonies were confirmed with a β-galactosidase assay. Selected clones were transformed into *E. coli*, isolated by antibiotic selection, and then the inserts were sequenced.

Pulldown Assays—^{35}S-Labeled proteins were synthesized *in vitro* using the TNT[regs] Coupled Wheat Germ Extract System (Promega). Labeled proteins were incubated with GST, recombinant GST-OsNug2, or GST-AtNug2, in buffer containing 50 mM Tris-HCl (pH 8.0), 1 mM EDTA, 150 mM NaCl, 0.1% Tween 20, and 0.5 mM DTT at room temperature for 1 h. The reaction mixture was then incubated with glutathione-agarose 4B beads at room temperature for 1 h. Beads were washed three times with the reaction buffer and then boiled in 50 μl of 2× SDS-PAGE sample buffer and subjected to electrophoresis on a 12% polyacrylamide gel. After electrophoresis, the gel was treated with Amplify (Amersham Biosciences), according to the manufacturer's instructions. Finally, the gel was dried and the signal was developed with a Cyclone PhosphorImager.

Transient Expression of GFP Fusion Proteins—Transformation of Oc cell protoplasts was used for transient expression of GFP and RFP fusion proteins in rice, according to the method described by Chen *et al.* (45). Fifteen micrograms of GFP- or RFP-fused DNA constructs were mixed with 100 μl of suspended protoplasts and then a 40% polyethylene glycol/Ca^{2+} solution (40% PEG 4000, 0.4 M mannitol, and 100 mM $CaCl_2$, adjusted to pH 7.0 with 1 M KOH) was added and mixed immediately by gentle shaking. Following a 20-min incubation at room temperature, 0.5 ml of W5 medium was added to dilute the PEG solution. Cells were incubated for a further 36 h in 1 ml of W5 solution at 22 °C. In the case of *Arabidopsis*, DNA encoding GFP and RFP fusion constructs (15 μg) were introduced into *Arabidopsis* protoplasts using the PEG-mediated transformation described previously (46). Transformed protoplasts were incubated at 22 °C for 48 h. Expression of fusion constructs was observed under a fluorescence microscope (Olympus AX70 TR, Olympus, Japan).

Preparation of Ribosomes and Sucrose Density Gradient Fractionation—Ribosomal profiles were performed according to the method described by Bassler *et al.* (26), with the following modification. Oc cells were subcultured in 100 ml of R2S suspension medium and grown for 10 days at 30 °C, under light and with shaking at 80 rpm. After washing in ice-cold breaking buffer (20 mM Tris-HCl, pH 8.0, 10 mM KCl, 2.5 mM $MgCl_2$, and 1 mM EGTA) containing 50 μg/ml of CHX, cells were harvested by centrifugation and resuspended in 10 ml of ice-cold breaking buffer containing 200 μg/ml of heparin and 1× complete protease inhibitors. Tungsten beads were added and cells were broken by five rounds of shaking for 2 min/resting for 2 min on ice, using a vibrating ball mill (Retsch, Germany). Cell debris was

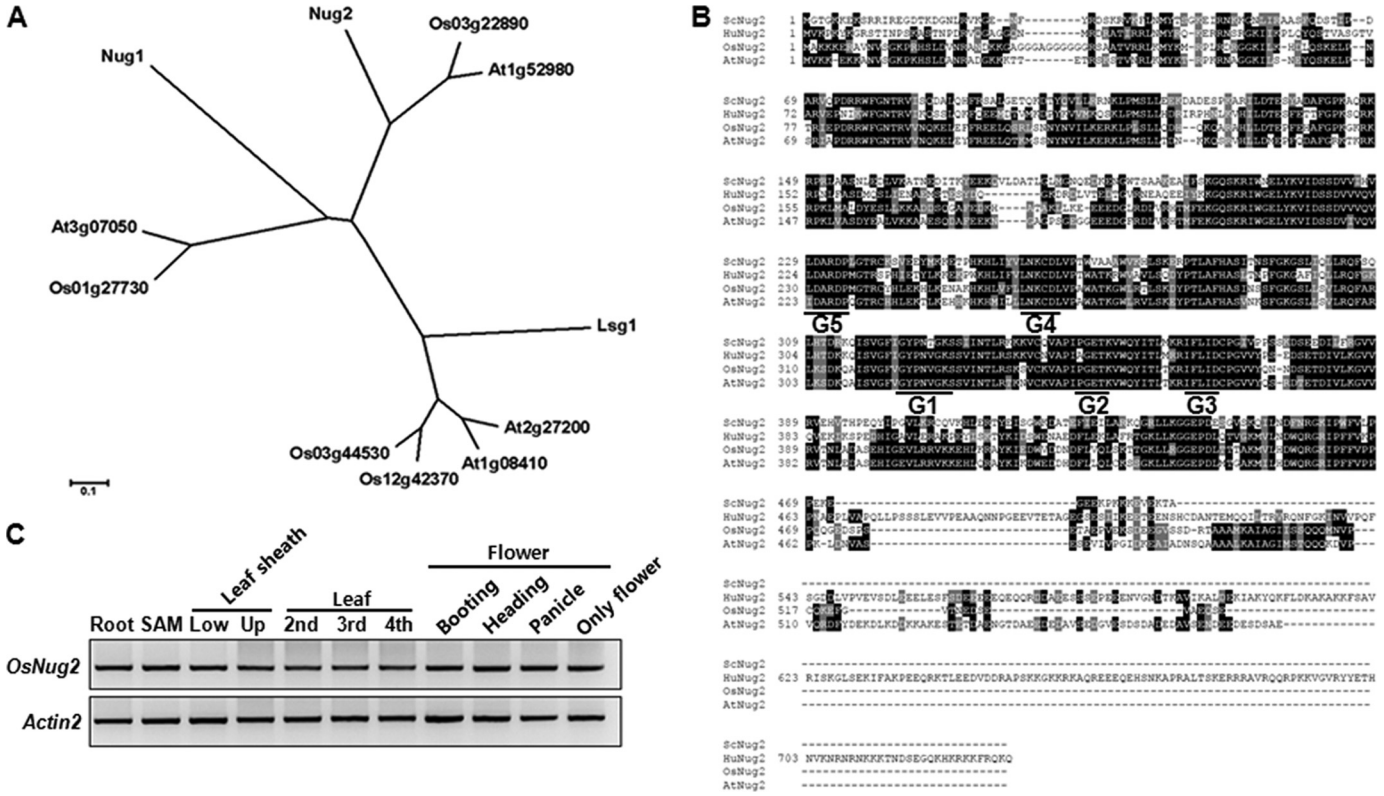

FIGURE 1. **Identification and expression patterns of YawG subfamily proteins in plants.** *A,* a phylogenetic tree of YawG subfamily proteins from rice and *Arabidopsis*. The phylogenetic tree was constructed with the neighbor-joining method, and visualized using the Molecular Evolutionary Genetics Analysis (MEGA 3.1) program. *B*, alignment of OsNug2 with amino acid sequences of other YawG homologues. GenBank™ accession numbers or Locus IDs in plants are: ScNug2 (*S. cerevisiae* Nug2); NP_014451, HsNug2 (*Homo sapiens* Nug2); NP_037417, Os03g22890, OsNug2 (*Oryza sativa* Nug2); and At1g52980, AtNug2 (*Arabidopsis thaliana* Nug2). *Black shading* indicates amino acids that match the consensus. *Gray shading* indicates amino acids similar to the consensus. The OsNug2 GTP-binding motifs (G1–G5) are *underlined*. *C, OsNug2* expression pattern in various tissues. Total RNAs were purified from the following tissues: 10-day-old roots, shoot apical meristem (*SAM*), leaf sheath (*LS*), 3-week-old leaf blade (*LB*), and flower from reproductive-phase plants. The *OsNug2* transcript level was determined using RT-PCR and gene-specific primers. *Actin2* transcripts were amplified as a quantitative control.

removed by centrifugation for 10 min at 14,000 × *g*. Approximately 20 OD_{260} units of cleared supernatant were loaded gently onto the top of sucrose gradients (7 to 47%) and then ultracentrifuged with a Beckman SW41 Ti rotor for 15 h at 200,000 × *g* at 4 °C. About 40 fractions (0.3 ml each) were collected and then examined for UV absorbance at OD_{260}. Each fraction was precipitated with 20% trichloroacetic acid (TCA) and 50% acetone, followed by resuspension in SDS loading buffer. Samples were separated by 12% SDS-PAGE and then subjected to immunoblotting with anti-OsNug2 or anti-human L10a antibodies. To determine the preferential form of OsNug2 bound to ribosomes, 2 mM GDP, GTP, and GTPγS or ATP, were added to cell lysates and incubated at 30 °C for 1 h prior to sucrose gradient fractionation.

RESULTS

Ubiquitous Expression of Two Plant Nug2 Genes Belonging to the YawG Subfamily and Isolated as Yeast Nug2 Orthologs—Yeast Nug1, Nug2, and Lsg1 amino acid sequences were used to query the rice and *Arabidopsis* genome databases to identify YawG subfamily orthologs (Fig. 1*A* and supplemental Table S1). Os03g22890 (*OsNug2*) and At1g52980 (*AtNug2*) were chosen for functional characterization as rice and *Arabidopsis* orthologs, respectively. The two plant Nug2s showed between 49 and 51% homology to the yeast proteins at the amino acid level (Fig. 1*B*). The GTP binding motifs in the middle domain were aligned in the order G5-G4-G1-G2-G3, which is consistent with the permuted feature typical of YawG proteins. In addition, RT-PCR analysis showed that *OsNug2* was expressed ubiquitously in all rice tissues analyzed (Fig. 1*C*). Similarly, analysis of the Genevestigator™ *Arabidopsis* microarray data base revealed that *AtNug2* is also expressed ubiquitously. These findings suggest that OsNug2 and AtNug2 might be essential at all stages of plant growth and development.

OsNug2 and AtNug2 Exhibit Intrinsic GTPase Activity, Which Is Stimulated by the Addition of 60S Ribosomal Subunits—GST-fused full-length *OsNug2* and *AtNug2* genes were expressed in *E. coli* and recombinant proteins were purified by GST affinity and gel-filtration chromatography. First, the GTP hydrolysis activities of these two proteins were analyzed using radioisotope-labeled [α-^{32}P]GTP. The GST-OsNug2 or GST-AtNug2 proteins were incubated with [α-^{32}P]GTP. Aliquots were withdrawn at appropriate time intervals and then separated on polyethyleneimine-cellulose TLC plates. The amount of GDP released by the two GST-fused Nug2s proteins increased gradually with time, indicating intact GTP hydrolysis activity *in vitro* (Fig. 2*A*). By contrast, the free GST control exhibited no GTP hydrolysis activity. In addition, the k_{cat} values of these two proteins were determined with a colorimetric

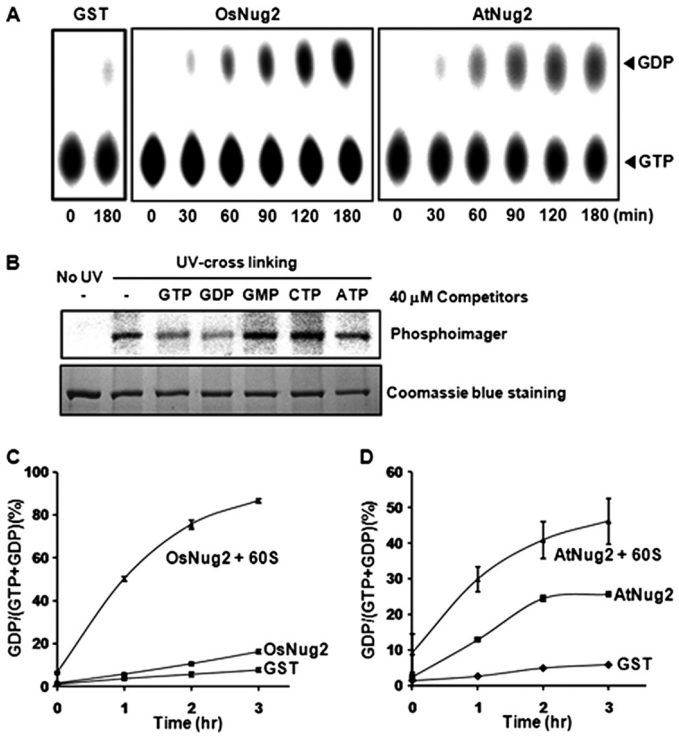

FIGURE 2. **GTP hydrolysis activity of OsNug2 and AtNug2 in the presence or absence of the 60S ribosomal subunit.** *A*, analysis of GTP hydrolysis activity. Reaction mixtures (100 μl) containing [α-^{32}P]GTP-radiolabeled GST-OsNug2 or GST-AtNug2 were incubated for 0 to 3 h. Aliquots were taken at various time points and GTPase activity was measured by separating the remaining GTP and GDP on a polyethyleneimine-cellulose TLC plate, followed by visualization with a Cyclone PhosphorImager. *B*, competition assay of the GST-OsNug2 protein. The purified GST-OsNug2 was first incubated with [α-^{32}P]GTP in reaction mixture, then, added excess amounts (400-fold) of the competing nucleotides indicated were incubated again under the same condition, prior to UV cross-linking. UV cross-linked OsNug2-[α-^{32}P]GTP complexes were visualized using a Cyclone PhosphorImager and then protein gel profiles were obtained after staining with Coomassie Brilliant Blue. *C* and *D*, GTP hydrolyzing activity of GST-OsNug2 or GST-AtNug2 is dependent upon the 60S ribosomal subunit. GTPase activity was measured by incubating 100 μl of reaction mixtures containing [α-^{32}P]GTP and the corresponding protein in the presence or absence of the 60S ribosomal subunit for 0 to 3 h. Sample aliquots (1 μl) were removed and separated by polyethyleneimine-TLC. To determine the GDP/(GTP + GDP) ratio (%), the relative intensities of GTP and GDP spots (*A*, *upper panels*) were calculated using OptiQuant software. The data represent the means of three independent experiments. *Error bars* represent mean ± S.D.

TABLE 1

The k_{cat} values of YlqF/YawG family

OsNug2 and AtNug2 mixed with 1 mM GTP and incubated 15 h at 30 °C. The released phosphate was measured. GST had no GTPase activity in this assay. Data represent mean ± S.D. or 4 or 6 independent experiments.

		k_{cat}	References
		min^{-1}	
OsNug2	*O. sativa*	0.12 ± 0.007 (n = 6)	This study
AtNug2	*A. thaliana*	0.087 ± 0.002 (n = 4)	This study
Nug1	*S. cerevisiae*	0.11 ± 0.01	28
YjeQ	*E. coli*	0.13	47

assay. The k_{cat} values of GST-OsNug2 and GST-AtNug2 were 0.12 ± 0.007 min^{-1} (n = 6) and 0.087 ± 0.002 min^{-1} (n = 4), respectively (Table 1). These values are similar to those of other YlqF/YawG family proteins examined previously in bacteria and yeast (21, 28, 47). Next, we also examined the ability of various nucleotides (*i.e.* GTP, GDP, GMP, ATP, and CTP) to compete for the binding of OsNug2 against [α-^{32}P]GTP (Fig. 2*B*). These results suggest that OsNug2 is a GTP/GDP-binding protein that is comparable with that of other YawG subfamily proteins.

TABLE 2

Stimulation of OsNug2 GTPase activity by ribosomal subunit

GTPase stimulation by ribosomal subunits was assessed by colorimetric assay. Reaction mixtures consisted of 3 μM OsNug2 and saturating levels of GTP (1 mM) in the presence or absence of ribosomal subunits (each 10 nM) for 15 h at 30 °C. GST had no GTPase activity in this assay. Data represent mean ± S.D. or 3 or 6 independent experiments.

	k_{cat}
	min^{-1}
OsNug2	0.12 ± 0.007 (n = 6)
OsNug2 + 40S subunit	0.123 ± 0.001 (n = 3)
OsNug2 + 60S subunit	0.178 ± 0.005 (n = 3)
OsNug2 + 80S ribosome	0.135 ± 0.004 (n = 3)

Interestingly, a few recent studies have shown that some GTPases play important roles in the ribosomal maturation process and that their GTPase activities are enhanced in the presence of ribosomal subunits *in vitro* (21, 25, 48). In light of these observations, we measured the kinetic parameters of OsNug2 hydrolytic activity in the presence 40S, 60S, or the 80S ribosome purified from rice. The intrinsic GTPase activity of OsNug2 was stimulated in the presence of ribosomes, particularly of the 60S ribosomal subunit (Table 2). Subsequently, GTPase activities of the Nug2 proteins were measured in the presence or absence of purified 60S ribosomal subunits obtained from Oc cells or *Arabidopsis* plants. As expected, addition of the cognate 60S subunit stimulated the GTPase activities of GST-OsNug2 and GST-AtNug2 by about 4- and 2-fold, respectively (Fig. 2, *C* and *D*). These findings suggest that 60S ribosomal subunits are required for effective GTP hydrolysis. Taken together, these findings suggest that the OsNug2 and AtNug2 proteins, which contain permuted GTPase motifs, exhibit intrinsic GTPase activity that can be stimulated by the addition of 60S ribosomal subunits.

OsNug2 Can Rescue the Lethality of a Yeast nug2 Null Mutant—Nug2 is a GTPase that is required during the late maturation stage of ribosomal pre-60S subunits (26, 27). To examine whether OsNug2 can function as a ribosomal GTPase in yeast, an *S. cerevisiae nug2* null mutant was used. Complementation analysis was dependent upon the viability of the haploid mutant yeast. A recombinant pYES2 plasmid containing the *OsNug2* cDNA under control of the *gal1* promoter was introduced into the diploid yeast mutant strain, *S. cerevisiae* Y26080 (*NUG2*/*nug2*::*KanMX4*), purchased from EUROSCARF (Fig. 3*A*, strain 2). The *nug2* deletion strain was obtained by sporulation and tetrad dissection. Transformants (Fig. 3*A*, strain 3) were divided into two haploid progenies, *i.e. nug2*::*kanMX4*/*GAL1*::*OsNug2* and *NUG2/GAL1*::*OsNug2* (Fig. 3*A*). The *nug2*::*kanMX4*/*GAL1*::*OsNug2* genotype (Fig. 3*A*, *strain 4*) was selected with synthetic complete medium without uracil (SC-U) and confirmed using SC-MU and/or SC-MUK medium with galactose, instead of glucose (Fig. 3*B*). Growth demonstrates that OsNug2 can complement the yeast *nug2* null mutation and therefore, rescue its lethality.

OsNug2 strain 4 (Fig. 3*A*) was used to investigate the role played by OsNug2 in rRNA processing during ribosomal maturation. Complementation analysis was performed by shifting

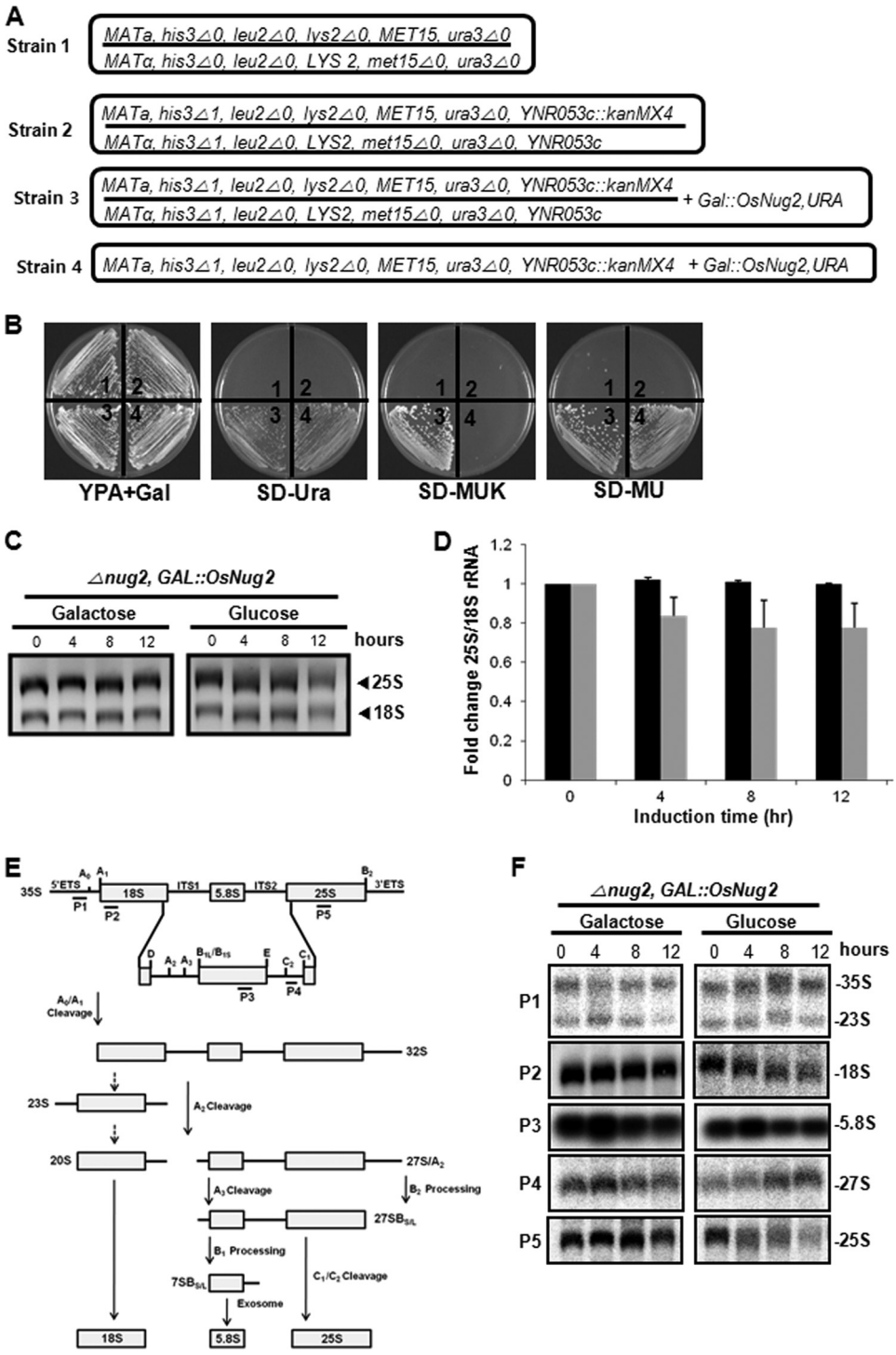

FIGURE 3. **OsNug2 complements the yeast *nug2* null mutation.** *A,* the strains used are as follows: *strain 1*, *S. cerevisiae* BY4743; *strain 2*, *S. cerevisiae* Y26080; *strain 3*, *S. cerevisiae* Y26080 with *Gal*::*OsNug2*; *strain 4*, *S. cerevisiae* Y26080 *nug2* null mutant with *Gal*::*OsNug2* from strain 3. *B,* the growth phenotype of strains 1–4 (numbered at the center of each sector in the Petri dish) were cultivated on different media. All media includes galactose. *C,* total RNAs were extracted at different time intervals from strain 4 cultures under OsNug2-inducible conditions on galactose-containing medium, and under OsNug2-suppression conditions on glucose-containing medium. Samples were separated on a 1.5% agarose-formaldehyde gel and stained with ethidium bromide. An equal amount (1 μg) of total RNA was loaded in each lane. *D,* the 25S/18S rRNA ratios are dependent upon induction time. The graph represents fold-changes in the 25S/18S rRNA ratio of Strain 4 cultured as described above for *C*, with OsNug2-inducible conditions (*black*) and OsNug2-suppression conditions (*gray*). These data were obtained from three independent experiments. *E,* schematic diagram showing the pre-rRNA and rRNA processing pathways in *S. cerevisiae*, and indicating the positions of hybridization probes. *F,* different RNAs were extracted from strain 4 cultured as described above in *C* and hybridized using gene-specific oligonucleotide probes. The probes used for RNA gel blot analysis are shown in *E* as P1 to P5 and were prepared as described previously (55). An equal amount (1 μg) of total RNA was loaded in each lane.

incubation of strain 4 at prescheduled time intervals, from a galactose-containing medium to medium with glucose for suppression of OsNug2 expression in the yeast *nug2* null mutant background. Cellular levels of 25S and 18S rRNAs decreased significantly according to the time elapsed after shifting to a glucose-containing medium (Fig. 3*C*). OsNug2-suppressed

cells showed a 10–20% reduction in the 25S/18S rRNA ratio compared with induced cells (Fig. 3*D*). The rRNA maturation pattern under OsNug2 suppression was examined using Northern blots hybridized with various intermediate rRNA size-specific oligonucleotide probes (Fig. 3*E*). The suppression of OsNug2 clearly reduced abundance of the 25S rRNA processed products and a weak reduction was also observed in 18S rRNA products (Fig. 3*F*). Transient weak accumulation of 27S pre-rRNA suggests that OsNug2 may be required at the late rRNA maturation step of large ribosomal subunit biogenesis. These findings, in addition to complementation of defective 25S rRNA maturation in the yeast *nug2* null mutant by OsNug2, support that OsNug2 is involved in pre-60S ribosomal maturation.

Two Plant Nug2 Proteins Are Targeted to the Nucleolus/Nucleus—Many steps in the ribosomal biogenesis process occur in the nucleolus and nucleoplasm, and various non-ribosomal factors involved in this process localize to these regions (13, 29, 49). Yeast Nug2 functions as a non-ribosomal factor that is targeted to both the nucleolus and nucleoplasm during the late stage of 60S subunit maturation (26, 27). To determine subcellular localization of OsNug2 in rice, a vector expressing the fluorescently tagged fusion protein GFP-OsNug2 was constructed (Fig. 4*A*). In addition, free GFP was used as a cytosolic reference control and a plasmid expressing the fusion protein RFP-NLS was generated as a nuclear reference. These constructs were introduced into rice protoplasts using the polyethylene glycol transformation method. Fusion proteins were observed by fluorescence microscopy. Free GFP was distributed uniformly in the cytoplasm, whereas OsNug2-GFP was targeted to the nucleolus/nucleus (Fig. 4, *B* and *C*). Similarly, AtNug2-GFP was introduced into *Arabidopsis* protoplasts and fluorescent signals were observed in the nucleolus/nucleus (supplemental Fig. S1). These findings indicate that plant Nug2s are nucleolus/nucleus-localized proteins.

OsNug2 Interacts Specifically with OsL10a, a Putative 60S Ribosomal Protein L10—To determine whether or not OsNug2 plays a role in the pre-60S ribosomal maturation process of rice, OsNug2 was used as bait to screen for potential partner proteins in a yeast two-hybrid rice cDNA library. Five clones were selected as potential OsNug2-interacting proteins (Table 3). One clone was predicted to encode L10a (Os08g44450), a putative 60S ribosomal protein L10; it was designated as OsL10a. A GST pulldown assay was performed to confirm the interaction between OsNug2 and OsL10a. GST-Nug2 interacted specifically with OsL10a *in vitro* (Fig. 5*B*). Moreover, a GST pulldown assay using GST-AtNug2 indicated that AtNug2 interacts with *Arabidopsis* L10a homologs (supplemental Fig. S2). Thus, it can be assumed that plant Nug2s may associate with the pre-60S ribosomal complex.

The N-terminal Region of OsNug2 Is Essential for Both Nucleolar/Nuclear Targeting and Association with OsL10a—As shown in Fig. 1*B*, the amino acid sequence alignment of various Nug2s indicates that OsNug2 comprises three domains: the N-terminal domain is well conserved among Nug2 orthologs, the middle domain contains a GTPase-fold with permuted G1-G5 motifs, and the C-terminal domain is of unknown function. Dissection analysis was performed to define the functions of these three domains. First, a GST pulldown assay was performed with full-length and/or various truncated forms of *in vitro* synthesized ^{35}S-labeled OsNug2 fragments, to determine the

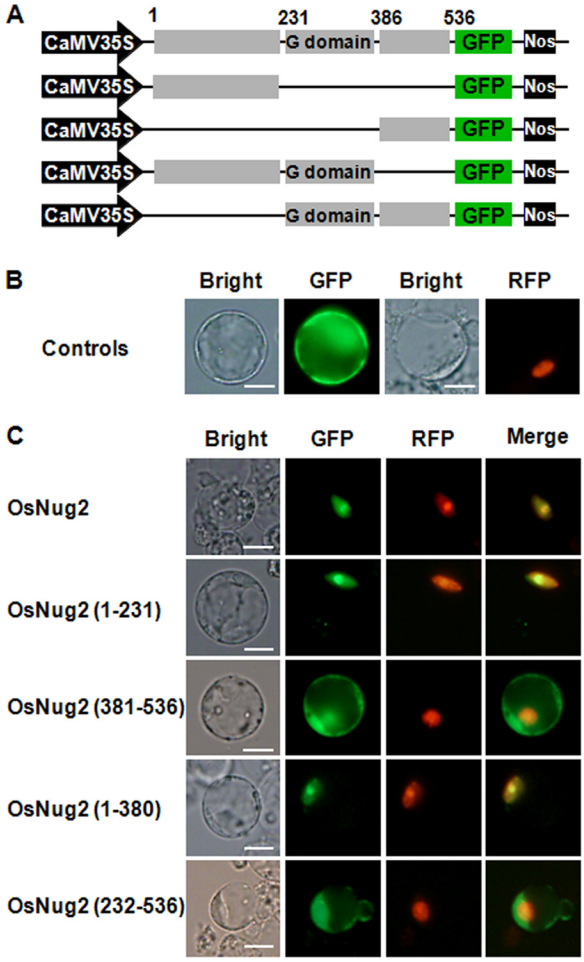

FIGURE 4. **Subcellular localization of OsNug2 deletion constructs.** *A*, schematic representation of GFP-OsNug2 and deletion constructs. *B*, rice protoplasts were transformed with vectors expressing GFP or NLS-RFP. Cells were incubated for 36 h and then observed by fluorescence microscopy. The *green* GFP signal was observed in the cytosol (*upper*, second image) and the *red* NLS-RFP signal was observed in the nucleus (*upper*, fourth image). *C*, colocalization analysis of GFP-OsNug2 deletion mutants with NLS-RFP. The number of amino acid residues is indicated in *parentheses* at the *left*. Rice protoplasts were transformed with vectors expressing GFP-OsNug2 fusion proteins and NLS-RFP. Fluorescence microscopy was used to analyze colocalization between the GFP-OsNug2 deletion mutants and NLS-RFP. OsNug2(Full)-GFP, OsNug2(1–231)-GFP, and OsNug2(1–380)-GFP were targeted to nucleolar/nucleolus; however, OsNug2(381–536)-GFP and OsNug2(232–536)-GFP were located to the cytoplasm. GFP (*green*) and RFP (*red*) signals indicate localization of OsNug2 and NLS fusions, respectively. *Merge* represents an overlaid image and overlap of OsNug2 and NLS generates a *yellow* color. *Bright* indicates a bright-field image. The *white bar* represents 10 μm.

TABLE 3

Five clones are predicted as interacting proteins by yeast two-hybrid screen

Gene index No.	Description[a]
Os08g44450	Putative 60S ribosomal protein L10a
Os05g06350	Putative import α-1b subunit
Os03g08460	Putative enthylene responsive element-binding protien
Os10g28610	Unknown protein, similar to centrosomal protein
Os01g61620	Putative ATP-binding protein, Ser-Thr protein kinase-like protein

[a] The cellular function was predicted based on Rice Genome Annotation Project.

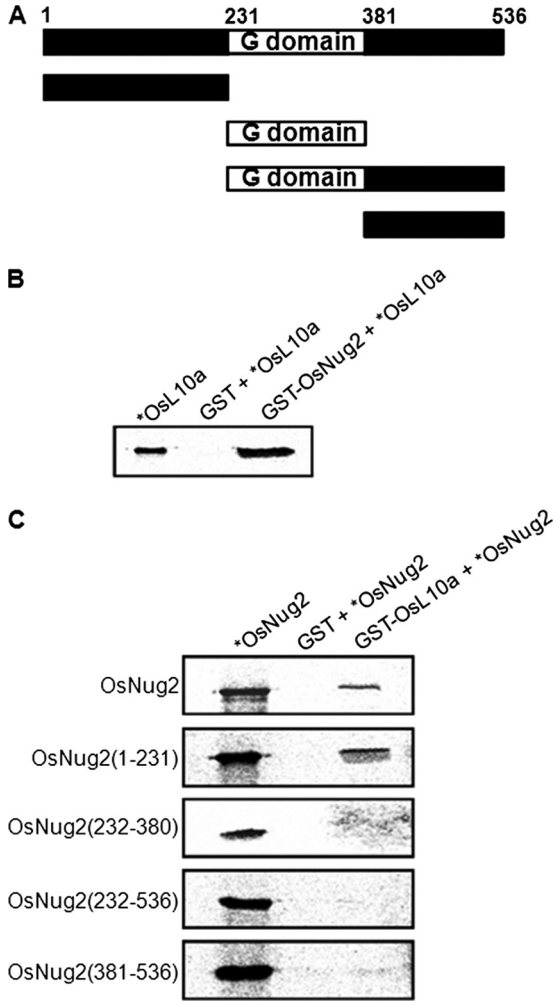

FIGURE 5. **Pulldown assays allow identification of the OsNug2 domain that interacts with OsL10a.** *A*, schematic representation of OsNug2 deletion variants. *B,* pulldown assay of GST-OsNug2 with [^{35}S]methionine-labeled OsL10a. Radiolabeled OsL10a was incubated with GST alone (*lane 2*) or GST-OsNug2 (*lane 3*). Reaction mixtures were incubated with glutathione beads, centrifuged, and the supernatants were discarded. Residual precipitates were boiled and subjected to SDS-PAGE. Five percent of total ^{35}S-labeled OsL10a was loaded into *lane 1* and 50% was used for the pulldown assay (*lane 3*). *C,* pulldown assay of [^{35}S]methionine-labeled OsNug2 deletion mutants with GST-OsL10a. Ten percent of total ^{35}S-labeled OsNug2 variants were loaded into *lane 1* and 50% was used for the pulldown assay (*lane 3*).

OsNug2 region responsible for interacting with OsL10a (Fig. 5*A*). GST-OsL10a was used as a probe. Only constructs expressing the N-terminal domain, *i.e.* full-length and OsNug2(1–231), showed binding to OsL10a, whereas constructs without the N-terminal region did not interact (Fig. 5*C*). These findings suggest that the N-terminal region of OsNug2 is responsible for interactions with OsL10a and the pre-60S ribosomal complex.

In addition, to define the region of OsNug2 responsible for nuclear localization, a few constructs expressing GFP-OsNug2 deletions were prepared (Fig. 4*A*) and introduced into rice protoplasts. The subcellular localization assay indicated that the N-terminal region is necessary for targeting OsNug2 to the nucleus (Fig. 4*C*).

OsNug2 Associates with the Pre-60S Ribosomal Subunit and Particularly Enhances Its Binding Affinity in the Presence of GTP—Because OsNug2 interacts with OsL10a, it is likely that at least these two proteins should be present in the pre-60S ribosomal complex. An RNA binding assay was performed to determine whether or not GST-OsNug2 associates with pre-60S rRNAs *in vitro*. GST-OsNug2 was mixed with total cell lysates from Oc cells. Following incubation, the mixture was affinity purified using glutathione-agarose 4B and then elutes were precipitated. Interactions between rRNA and OsNug2 were identified by hybridization with probes against specific rRNAs such as 5S, 5.8S, 18S, and 25S rRNA. GST-OsNug2 bound 25S, 5.8S, and 5S rRNA, but no interactions were detected with 18S rRNA (Fig. 6*A*). These suggest that OsNug2 associates with the pre-60S ribosomal complex, which consists of 5S, 5.8S, and 25S rRNA.

Next, we investigated whether or not OsNug2 associates with intranuclear pre-60S ribosomal protein particles, and if so, which part of ribosome is involved in this association. Whole cell lysates were prepared from Oc cells, fractionated by 7 to 47% sucrose density gradient centrifugation and then fractions were separated by 12% SDS-PAGE. Cofractionation of OsNug2 with ribosomal subunits was visualized by immunoblotting with anti-OsNug2 antibody. The ribosomal complex $OD_{260\ nm}$ profile showed distinct separation of the 40S and 60S ribosomal subunits, 80S whole ribosome and polysomes (Fig. 6*B*). Immunoblotting data in Fig. 6*B* shows that OsNug2 cosedimented with the 60S large ribosomal subunit; however, it was not associated with the 80S complex or with polysomes. These findings imply that OsNug2 functions exclusively in pre-60S ribosomal subunit maturation. Anti-human L10a antibody was used as a sedimentation control for identification of the 60S ribosomal subunit fraction, because human L10a shows 60% homology with OsL10a. Fractions containing OsNug2 and OsL10a overlapped with the 60S ribosomal subunit fraction (Fig. 6*B*). This finding is consistent with results obtained in the yeast two-hybrid and pulldown assays, and provides further support for the suggestion that OsNug2 associates with the rice pre-60S ribosomal complex via a ribosomal OsL10a protein. It is noteworthy that the major OsNug2 signal was detected from the top of the gradient, indicating that most OsNug2 is not bound to ribosomes. This finding implies that OsNug2 dissociates from the pre-60S ribosomal particle prior to ribosomal assembly into the functional 80S complex, a hypothesis consistent with the suggestion that OsNug2 functions as a non-ribosomal factor in the nucleus/nucleolus, prior to ribosomal export to the cytoplasm.

Finally, the influence of guanine nucleotides on the OsNug2-ribosome interaction was investigated. Oc cell lysates were incubated in the presence or absence of excess guanine nucleotides and then fractionated using sucrose density gradient centrifugation. Immunoblot analysis with anti-OsNug2 antibody indicates that OsNug2 interacts with the 60S ribosomal subunit in the presence of GTP, GDP, GTPγS, and ATP (Fig. 6*C*). For quantitative interpretation, the relative fold-changes, which represent the ratio of the precipitated amounts of OsNug2-bound 60S ribosomal subunits in the presence of diverse nucleotides against that of control, from the immunoblot staining experiment were calculated. As shown in Fig. 6*D*, GTP-bound OsNug2 shows the highest binding affinity with 60S ribosomal subunits, contrary to other nucleotides including GDP. It suggests that the association between OsNug2 and

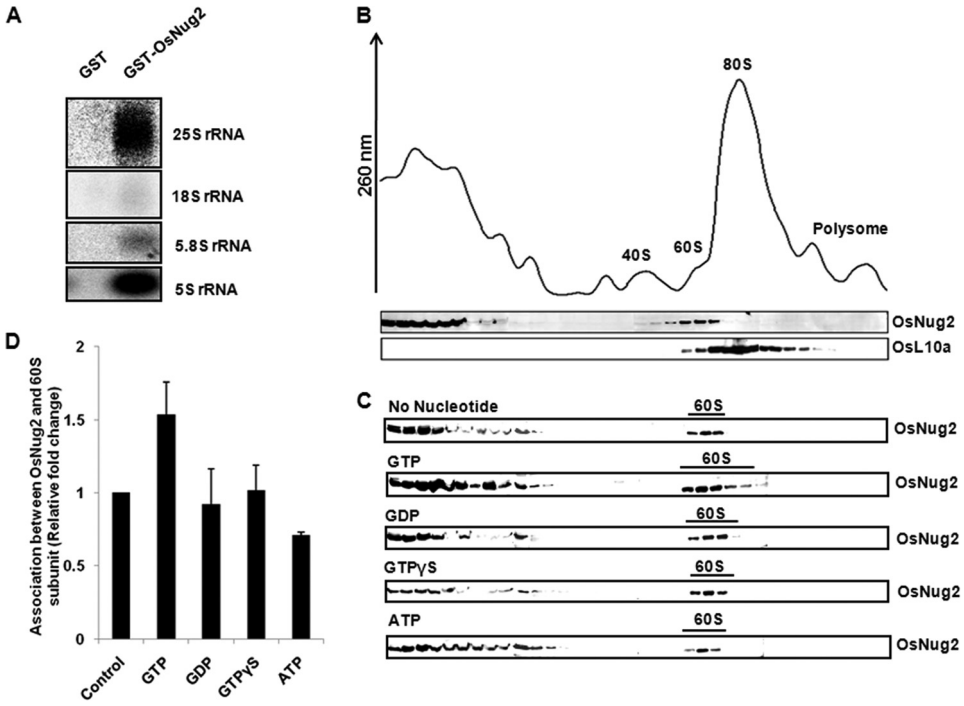

FIGURE 6. **Association between OsNug2 and ribosomal subunits in the presence of various nucleotides.** *A,* rRNA binding assay. GST or GST-OsNug2 was mixed with total Oc cell lysate and the mixture incubated with glutathione-agarose 4B. Following centrifugation, the supernatant was discarded. Residual precipitates were treated with phenol to obtain rRNAs. Isolated rRNAs were separated on a 15% formaldehyde-agarose gel and then hybridization was performed using specific rRNAs as probes. *B,* whole cell lysates from Oc cells were sedimented through 7–47% sucrose gradients. The UV profiles at $OD_{260\ nm}$ of individual fractions show 40S and 60S subunits, 80S whole ribosomes and polysomes. The *upper column* under the UV profile graph represents that after the TCA precipitation, an equal volume of proteins from each fraction were analyzed by SDS-PAGE and immunoblotted with anti-OsNug2 antibody. In the next column, the 60S ribosomal subunit was detected with anti-human L10a antibody, instead of OsL10a. *C,* ribosomal subunits in the presence of 2 mM GTP, GDP, GTPγS, or ATP, were sedimented through 7–47% sucrose gradients, as described in *B*. *D,* relative fold-changes of association between OsNug2 and 60S ribosomal subunits. The data represent the means of three independent measurements. *Error bars* represent mean ± S.D.

the pre-60S ribosomal subunit can be enhanced by the addition of GTP.

AtNug2-mediated Maturation of Pre-60S Ribosomal Subunits May Be Linked to Translational Efficiency—In view of having GTPase activity, it is of interest to determine what is the main role of OsNug2 in the pre-60S ribosomal subunit maturation process of plant. To investigate its physiological role, a Nug2-defective mutant was constructed by silencing the *AtNug2* gene using RNAi. A 500-bp fragment of *AtNug2* cDNA was generated by RT-PCR and then inserted into vector pFGC1008 with sense and antisense orientations linked by a 300-bp partial *GUS* gene (Fig. 7*A*). The recombinant vector was introduced into *A. tumefaciens* strain LBL4404, which was then used to transform to Col-0 plants via the floral dip method. Eight hygromycin-resistant transformants were selected. Two independent lines, $AtNug2^{RNAi\text{-}5}$ and $AtNug2^{RNAi\text{-}6}$, showed significantly reduced *AtNug2* expression (Fig. 7*B*). Transcription levels were normalized against *Actin2*.

If AtNug2 activates the 60S ribosomal subunit for translation, it might be expected that mutants carrying a deleted or mutated *AtNug2* gene would exhibit problems with translation and show hypersensitivity to a translational inhibitor that interacts directly with the ribosome. To determine whether or not AtNug2 is required to facilitate the late stage of pre-60S rRNAs maturation, the CHX sensitivity of *AtNug2* RNAi mutants was examined. WT and *AtNug2* RNAi mutants were germinated on MS/2 plates and then 10-day-old seedlings were transferred to MS plates containing 0.2–1.6 μM CHX. After 2 weeks growth on CHX-containing medium, both *AtNug2* RNAi mutant lines showed substantially reduced growth and more developmental abnormalities than WT (Fig. 7*C*). The *AtNug2* RNAi mutant lines exhibited expanded green or purple leaves and yellow or light-brown cotyledons, which suggests a lack of translational efficiency caused by defective pre-60S ribosomal subunit processing. For quantitative assessment of CHX sensitivity, relative fresh weights (FW) were measured from seedlings grown for 2 weeks on MS/2 plates containing various concentrations of CHX. On medium containing 0.4 μM CHX, the RNAi mutants $AtNug2^{RNAi\text{-}5}$ and $AtNug2^{RNAi\text{-}6}$ showed the greatest CHX sensitivity, with about a 40% reduction in FW relative to WT (Fig. 7*D*). These findings indicate that AtNug2 is involved in pre-60S ribosomal subunit maturation and thus, it might be linked to translational efficiency of the ribosome.

AtNug2 Is Expressed Ubiquitously throughout the Plant and Most Strongly in Meristematic Regions—To examine the spatial expression pattern of *AtNug2*, ~1.5-kb fragment from the *AtNug2* promoter region was inserted in front of a transcriptional reporter gene (*GUS*) in pCAMBIA1381. After transformation of this recombinant plasmid into *Arabidopsis*, numerous hygromycin-resistant plants were selected. T2 generation seedlings from 12 independent transgenic lines were analyzed by histochemical staining for GUS activity. The expression profiles of all lines were

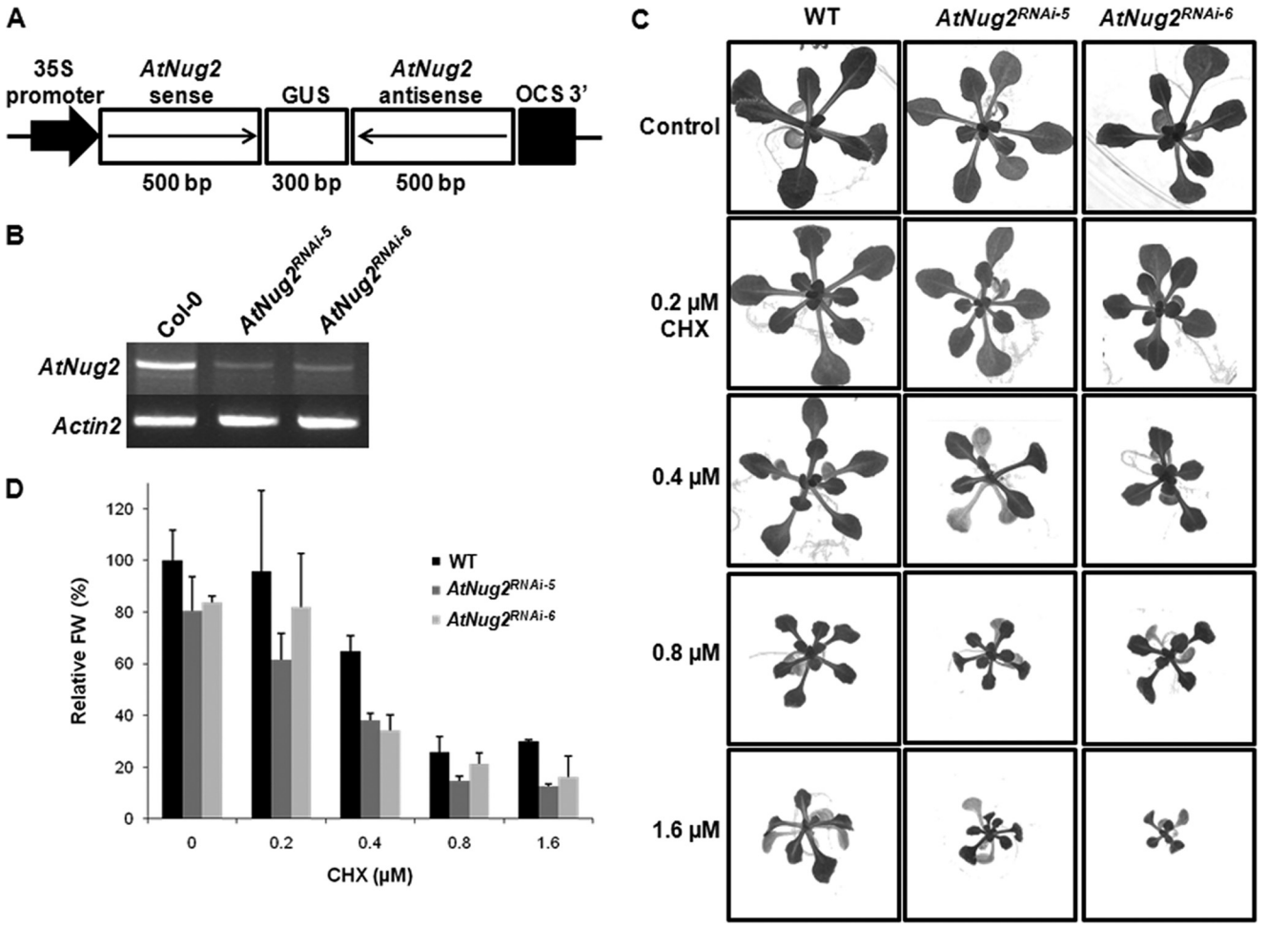

FIGURE 7. **CHX sensitivity of two *AtNug2* RNAi mutants.** *A,* mutants *AtNug2*$^{RNAi-5}$ and *AtNug2*$^{RNAi-6}$ were constructed by inserting a 500-bp *AtNug2* target sequence in sense and antisense orientations, and linked by a 300-bp partial *GUS* gene. The ^{35}S-promoter (from the Cauliflower mosaic virus ^{35}S-promoter) and OCS region are shown. *B,* RT-PCR analysis of *AtNug2* expression in Col-0 and T2 progeny of RNAi transgenic plants. RNAs were isolated from whole plants 2 weeks after germination. The two RNAi transgenic plants show a marked reduction in *AtNug2* transcript levels, but not in *Actin2* expression. *C,* phenotypes of WT seedlings and RNAi mutants grown on MS/2 medium containing different concentrations of CHX. Ten-day-old seedlings germinated on MS/2 plates were transferred to CHX-containing medium and grown for a further 2 weeks. *D,* relative percentage FW of 2-week-old plants is dependent upon the concentration of CHX. Each data set represents the means of five independent measurements. *Error bars* represent the mean ± S.D.

similar. Histochemical staining revealed that the *AtNug2* promoter::*GUS* construct was expressed throughout entire plants (Fig. 8, *B–D*), contrary to the 30-day-old WT exhibiting no GUS activity (Fig. 8*A*). Strong GUS staining localized at the primary root tip and elongating zone (Fig. 8, *C* and *D*, respectively). In 3-week-old plants, GUS staining was also distributed throughout the entire plant, with strong expression in the cotyledon, vascular veins of rosette leaves, and lateral root tip (Fig. 8, *E–H*). However, staining was not detected in epidermal or cortical cells of the root (Fig. 8*H*). In 30-day-old plants, strong GUS activity was observed in the elongation region of floral organs and cauline leaves (Fig. 8, *I* and *K*). Mature siliques typically displayed additional staining, with a stronger staining pattern at both ends (Fig. 8*J*). In all plants analyzed, the vascular systems stained very intensely in the roots (Fig. 8, *C*, *G*, and *H*), most leaves (Fig. 8, *F* and *K*), silique stems (Fig. 8*J*), and several floral organs (Fig. 8*I*). These data suggest that *AtNug2* is expressed ubiquitously throughout the plant and most strongly in meristematic regions.

DISCUSSION

Ribosome is the submicroscopic machinery that synthesizes proteins in organisms and the biogenesis of ribosome is a very complicated process that involves many ribosomal and non-ribosomal factors. Recently, it has been reported that GTPases represent the largest class of non-ribosomal factors involved in ribosome biogenesis (11). The YlqF/YawG family belong to the P-loop GTPases, which are characterized by a permuted order of GTPase motifs within the G-binding domain, a feature that is highly conserved among diverse organisms from bacteria to humans (1, 20). Although YawG subfamily proteins have not been extensively studied in plants, these proteins are relatively well characterized in yeast and mammalian systems, where they have been implicated in biogenesis of the 60S ribosomal subunit (26, 27, 29, 30, 49). A few genes have been identified as encoding putative YawG subfamily GTPases in *Arabidopsis* and rice (Fig. 1*A* and supplemental Table S1). This is the first report examining the physiological role played by plant Nug2 proteins. These proteins belong to the YawG subfamily of

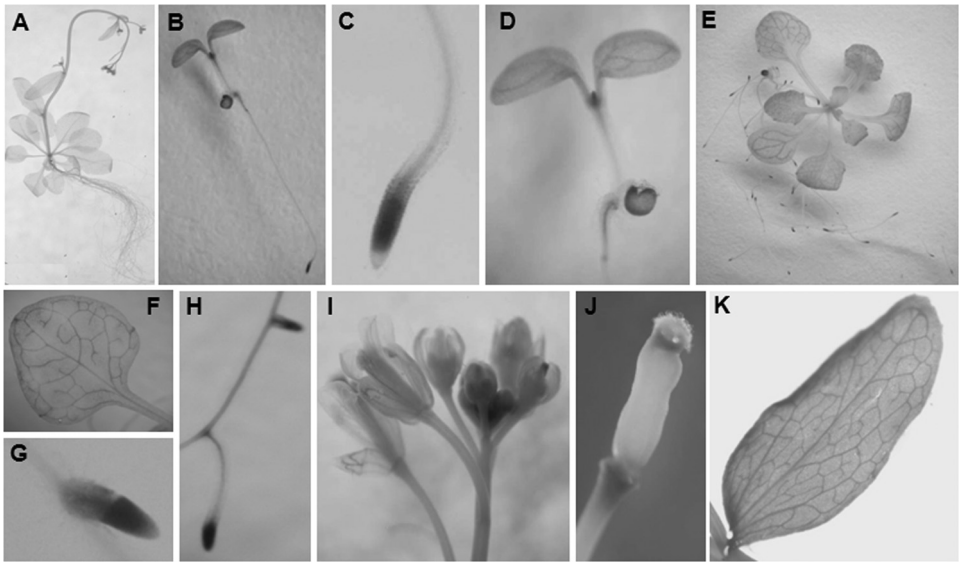

FIGURE 8. **AtNug2 promoter-*GUS* expression patterns in transgenic *Arabidopsis* plants.** The 1,500-bp *AtNug2* gene promoter was inserted upstream of the GUS coding sequence in expression vector pCAMBIA1381. The *AtNug2* promoter:*GUS* construct was introduced into *A. tumefaciens* strain LBL4404, which was then used to transform Col-0 plants by the floral dip method. Transgenic plants were selected and used for GUS activity assays. *A,* 30-day-old WT. *B,* 5-day-old whole seedlings. *C,* primary root tip of 5-day-old seedlings. *D,* meristematic regions of 5-day-old seedlings. *E,* 3-week-old whole seedlings. *F,* rosette leaf from a 3-week-old plant. *G,* lateral root tip from a 3-week-old plant. *H*, 3-week-old root stem and lateral root tip. *I,* flowers. *J,* mature silique. *K,* caulin leaf.

GTPases and interact directly with OsL10a, a putative ribosomal factor in the large subunit complex.

To determine whether or not the Nug2 proteins isolated from *Arabidopsis* and rice can function as GTPases during 60S ribosomal subunit maturation, the intrinsic GTPase activities were measured using phosphorimaging and GDP/GTP + GDP ratios (%). As shown in Fig. 2, *C* and *D*, the GTPase activity of these proteins was greatly enhanced by the presence of the 60S ribosomal subunit. Moreover, OsNug2 expression can rescue the lethal yeast *nug2* null mutation by complementing a defect in 25S rRNA maturation. OsNug2 and AtNug2 are also localized to the nucleolus/nucleus (Figs. 3 and 4). These findings suggest strong conservation of the functional role played by Nug2 proteins in mono- and dicotyledenous plants (26, 27).

A yeast two-hybrid assay was used to identify partner proteins that interact with OsNug2. A putative 60S ribosomal protein L10a (*Os08g44450*) was identified among the five positive clones encoding potential interaction partners (Table 3). OsNug2 associates with pre-60S particles (Fig. 5*B*) and it appears that the N-terminal region of OsNug2 is essential for this association (Fig. 5*C*). Fractionation analysis revealed that OsNug2 showed the highest binding affinity to ribosomes in the presence of GTP, but binding was not as strong in the presence of other nucleotides or guanine nucleotide derivatives (Fig. 6*C*). To examine the effect of OsNug2 on growth retardation, the relative fresh weights (FW) of RNAi knockdown mutants $AtNug2^{RNAi\text{-}5}$ and $AtNug2^{RNAi\text{-}6}$ were examined. Growth of the knockdown mutants were reduced with increasing concentrations of CHX (Fig. 7*D*). Finally, analysis of the *AtNug2* expression pattern revealed that it was expressed ubiquitously in plants and most strongly in the meristematic regions.

Recently, a few studies have reported that YawG subfamily proteins contain three domains, *i.e.* unique N- and C-terminal regions flanking a conserved GTPase domain in the middle region (20, 21, 26, 28). The functions of these domains are becoming better understood. For example, the N-terminal region of Nug1 is important for association with pre-60S ribosomal particles, RNA binding, and localization to the nucleolus/nucleus, whereas the middle domain comprises a circularly permuted GTPase-fold with intrinsic GTP hydrolysis activity (28). Here, subcellular localization and pulldown assays demonstrated that the N-terminal region of OsNug2 is essential for nucleolar/nuclear targeting and for binding OsL10a (Figs. 4 and 5). These results imply that the N-terminal region of Nug proteins is broadly conserved among eukaryotes and that it plays a critical role in protein-protein or protein-RNA interactions, as well as in targeting to the nucleolus/nucleus.

The yeast two-hybrid system identified the putative 60S ribosomal protein L10a as an interaction partner of OsNug2 (Table 3). Pulldown assays using various *OsNug2* deletion constructs confirmed direct interaction between L10a and the N terminus of OsNug2 (Fig. 5*C*). L10a is an ortholog of *E. coli* L1 and it is highly conserved from prokaryotes to eukaryotes; however, its detailed function is not yet clearly defined. In prokaryotes, a few reports have proposed that L1 may function in protein synthesis by releasing deacylated tRNAs through the ribosomal E site in *E. coli* (50). In plants, abnormal patterning in development has been linked to mutations in several genes encoding 60S ribosomal proteins, including *Arabidopsis* L10a, an ortholog of OsL10a (38). It is possible that OsNug2 controls incorporation of OsL10a into the 60S ribosomal subunit, potentially regulating formation of complete 80S ribosomes. However, investigation of this hypothesis will require further elucidation of the mechanisms underlying the interaction between OsNug2 and OsL10a.

Sprang (51) proposed that stimulation of GTP hydrolysis by a GTPase-activating protein may occur through the facilitation of a conformational change in the G-protein molecule or its interaction partner. Previous studies have shown that the addition of exogenous nucleotides can change the association pat-

terns of several small GTPases, including RsgA (YjeQ), CgtAE, and HflX (16, 21, 52), increasing GTPase activities in the presence of ribosomal subunits. YlqF, an ortholog of OsNug2 in prokaryotes, binds free 50S subunits in the presence of GTPγS and its GTPase activity is strongly stimulated by the addition of 50S subunits *in vitro* (25). Here, the fractionation assay showed that OsNug2 proteins associate predominantly with the 60S ribosomal subunit and not the 40S subunit, mature 80S, or polysomes (Fig. 6*B*). These findings indicate that OsNug2 is associated exclusively with the large 60S ribosomal subunit. Moreover, this interaction is strongly facilitated by the presence of GTP, but not other nucleotides or guanine nucleotide derivatives such as ATP, GDP, or GTPγS (Fig. 6*C*). The GTPase activity of plant Nug2 was also enhanced significantly by addition of the 60S ribosomal subunit (Fig. 2*B*). Taken together, these results suggest a model for interaction between OsNug2 and the 60S ribosomal subunit. Once GTP-bound OsNug2 binds to the 60S ribosomal subunit, conformational changes are induced in the large subunit, and it leads to enhancement of GTP hydrolysis during such an interaction, and subsequently GDP-bound OsNug2 is produced. This hydrolytic product would be dissociated immediately prior to export of the ribosome to the cytoplasm. To determine whether this model is correct, the molecular mechanism through which OsNug2 GTPase is activated by association with ribosomal subunits should be elucidated.

Previous studies have reported that recessive alleles of YawG subfamily genes are responsible for severe growth and developmental abnormalities, which are caused by defective 60S ribosomal subunit maturation (25, 27). Furthermore, mutant cells deficient in ribosomal biogenesis or translation processes showed translational disorders and hypersensitivity to aminoglycoside antibiotics/translational inhibitors (53, 54). Here, hypersensitivity to translational inhibitors was examined using CHX, which interferes with the translocation step of translation. As expected, the relative FWs of two *AtNug2* RNAi mutants decreased more significantly with increasing concentrations of CHX than that of WT (Fig. 7, *C* and *D*). The reduced fresh weight and defective pleiotrophic phenotypes caused by CHX treatments suggest that the *AtNug2* mutation leads to inefficient 60S ribosomal complex maturation and translational inhibition, which eventually present as growth retardation and developmental defects. Moreover, histochemical staining revealed that *AtNug2* is expressed ubiquitously in the plant, but is showing higher expression in meristematic regions (Fig. 8).

In conclusion, this study provides important insights into the expression and functions of plant Nug2 proteins as the nonribosomal factors. In the presence of GTP, Nug2 proteins associate strongly with the pre-60S large ribosomal subunit complex. Efficient maturation of the pre-60S ribosomal subunit is required for association with the 40S ribosomal subunit in the cytosol, allowing assembly of a complete 80S ribosome. Based on this, Nug2 GTPase activity appears to be critical for normal growth and development of plants.

Acknowledgments—We thank Soon Ju Park and Hae Ryong Park, Gyeongsang National University, Korea, for technical assistance in using rice Oc cells.

REFERENCES

1. Fromont-Racine, M., Senger, B., Saveanu, C., and Fasiolo, F. (2003) *Gene* **313,** 17–42
2. Venema, J., and Tollervey, D. (1999) *Annu. Rev. Genet.* **33,** 261–311
3. Tschochner, H., and Hurt, E. (2003) *Trends Cell Biol.* **13,** 255–263
4. Warner, J. R. (2001) *Cell* **107,** 133–136
5. Kressler, D., Linder, P., and de la Cruz, J. (1999) *Mol. Cell. Biol.* **19,** 7897–7912
6. Grandi, P., Rybin, V., Bassler, J., Petfalski, E., Strauss, D., Marzioch, M., Schäfer, T., Kuster, B., Tschochner, H., Tollervey, D., Gavin, A. C., and Hurt, E. (2002) *Mol. Cell* **10,** 105–115
7. Granneman, S., and Baserga, S. J. (2004) *Exp. Cell Res.* **296,** 43–50
8. Zemp, I., and Kutay, U. (2007) *FEBS Lett.* **581,** 2783–2793
9. Nissan, T. A., Bassler, J., Petfalski, E., Tollervey, D., and Hurt, E. (2002) *EMBO J.* **21,** 5539–5547
10. Dutca, L. M., and Culver, G. M. (2005) *Mol. Cell* **20,** 497–499
11. Karbstein, K. (2007) *Biopolymers* **87,** 1–11
12. Schaefer, L., Uicker, W. C., Wicker-Planquart, C., Foucher, A. E., Jault, J. M., and Britton, R. A. (2006) *J. Bacteriol.* **188,** 8252–8258
13. Karbstein, K., Jonas, S., and Doudna, J. A. (2005) *Mol. Cell* **20,** 633–643
14. Bharat, A., Jiang, M., Sullivan, S. M., Maddock, J. R., and Brown, E. D. (2006) *J. Bacteriol.* **188,** 7992–7996
15. Sato, A., Kobayashi, G., Hayashi, H., Yoshida, H., Wada, A., Maeda, M., Hiraga, S., Takeyasu, K., and Wada, C. (2005) *Genes Cells* **10,** 393–408
16. Jain, N., Dhimole, N., Khan, A. R., De, D., Tomar, S. K., Sajish, M., Dutta, D., Parrack, P., and Prakash, B. (2009) *Biochem. Biophys. Res. Commun.* **379,** 201–205
17. Muench, S. P., Xu, L., Sedelnikova, S. E., and Rice, D. W. (2006) *Proc. Natl. Acad. Sci. U.S.A.* **103,** 12359–12364
18. Wicker-Planquart, C., Foucher, A. E., Louwagie, M., Britton, R. A., and Jault, J. M. (2008) *J. Bacteriol.* **190,** 681–690
19. Sayed, A., Matsuyama, S., and Inouye, M. (1999) *Biochem. Biophys. Res. Commun.* **264,** 51–54
20. Leipe, D. D., Wolf, Y. I., Koonin, E. V., and Aravind, L. (2002) *J. Mol. Biol.* **317,** 41–72
21. Daigle, D. M., and Brown, E. D. (2004) *J. Bacteriol.* **186,** 1381–1387
22. Campbell, T. L., Daigle, D. M., and Brown, E. D. (2005) *Biochem. J.* **389,** 843–852
23. Uicker, W. C., Schaefer, L., Koenigsknecht, M., and Britton, R. A. (2007) *J. Bacteriol.* **189,** 2926–2929
24. Uicker, W. C., Schaefer, L., and Britton, R. A. (2006) *Mol. Microbiol.* **59,** 528–540
25. Matsuo, Y., Morimoto, T., Kuwano, M., Loh, P. C., Oshima, T., and Ogasawara, N. (2006) *J. Biol. Chem.* **281,** 8110–8117
26. Bassler, J., Grandi, P., Gadal, O., Lessmann, T., Petfalski, E., Tollervey, D., Lechner, J., and Hurt, E. (2001) *Mol. Cell* **8,** 517–529
27. Saveanu, C., Bienvenu, D., Namane, A., Gleizes, P. E., Gas, N., Jacquier, A., and Fromont-Racine, M. (2001) *EMBO J.* **20,** 6475–6484
28. Bassler, J., Kallas, M., and Hurt, E. (2006) *J. Biol. Chem.* **281,** 24737–24744
29. Kallstrom, G., Hedges, J., and Johnson, A. (2003) *Mol. Cell Biol.* **23,** 4344–4355
30. Hedges, J., West, M., and Johnson, A. W. (2005) *EMBO J.* **24,** 567–579
31. Byrne, M. E. (2009) *Trends Plant Sci.* **14,** 512–519
32. Giavalisco, P., Wilson, D., Kreitler, T., Lehrach, H., Klose, J., Gobom, J., and Fucini, P. (2005) *Plant Mol. Biol.* **57,** 577–591
33. McIntosh, K. B., and Bonham-Smith, P. C. (2005) *Genome* **48,** 443–454
34. Degenhardt, R. F., and Bonham-Smith, P. C. (2008) *Plant Physiol.* **147,** 128–142
35. Wood, A. J., Joel Duff, R., and Oliver, M. J. (2000) *J. Exp. Bot.* **51,** 1655–1662
36. Nishimura, T., Wada, T., Yamamoto, K. T., and Okada, K. (2005) *Plant Cell* **17,** 2940–2953
37. Popescu, S. C., and Tumer, N. E. (2004) *Plant J.* **39,** 29–44
38. Pinon, V., Etchells, J. P., Rossignol, P., Collier, S. A., Arroyo, J. M., Martienssen, R. A., and Byrne, M. E. (2008) *Development* **135,** 1315–1324

39. Petricka, J. J., and Nelson, T. M. (2007) *Plant Physiol.* **144,** 173–186
40. Pontvianne, F., Matía, I., Douet, J., Tourmente, S., Medina, F. J., Echeverria, M., and Sáez-Vásquez, J. (2007) *Mol. Biol. Cell* **18,** 369–379
41. Baba, A., Hasezawa, S., and Syono, K. (1986) *Plant Cell Physiol.* **27,** 463–471
42. Furukawa, T., and Syono, K. (1998) *Plant Cell Physiol.* **39,** 43–48
43. Jefferson, R. A., Kavanagh, T. A., and Bevan, M. W. (1987) *EMBO J.* **6,** 3901–3907
44. Seo, H. S., Choi, C. H., Kim, H. Y., Jeong, J. Y., Lee, S. Y., Cho, M. J., and Bahk, J. D. (1997) *Eur. J. Biochem.* **249,** 293–300
45. Chen, S., Tao, L., Zeng, L., Vega-Sanchez, M. E., Umemura, K., and Wang, G. L. (2006) *Mol. Plant Pathol.* **7,** 417–427
46. Heo, J. B., Rho, H. S., Kim, S. W., Hwang, S. M., Kwon, H. J., Nahm, M. Y., Bang, W. Y., and Bahk, J. D. (2005) *Plant Cell Physiol.* **46,** 2005–2018
47. Daigle, D. M., Rossi, L., Berghuis, A. M., Aravind, L., Koonin, E. V., and Brown, E. D. (2002) *Biochemistry* **41,** 11109–11117
48. Matsuo, Y., Oshima, T., Loh, P. C., Morimoto, T., and Ogasawara, N. (2007) *J. Biol. Chem.* **282,** 25270–25277
49. Du, X., Rao, M. R., Chen, X. Q., Wu, W., Mahalingam, S., and Balasundaram, D. (2006) *Mol. Biol. Cell* **17,** 460–474
50. Fei, J., Kosuri, P., MacDougall, D. D., and Gonzalez, R. L., Jr. (2008) *Mol. Cell* **30,** 348–359
51. Sprang, S. R. (1997) *Annu. Rev. Biochem.* **66,** 639–678
52. Jiang, M., Datta, K., Walker, A., Strahler, J., Bagamasbad, P., Andrews, P. C., and Maddock, J. R. (2006) *J. Bacteriol.* **188,** 6757–6770
53. Himeno, H., Hanawa-Suetsugu, K., Kimura, T., Takagi, K., Sugiyama, W., Shirata, S., Mikami, T., Odagiri, F., Osanai, Y., Watanabe, D., Goto, S., Kalachnyuk, L., Ushida, C., and Muto, A. (2004) *Nucleic Acids Res.* **32,** 5303–5309
54. Menne, T. F., Goyenechea, B., Sánchez-Puig, N., Wong, C. C., Tonkin, L. M., Ancliff, P. J., Brost, R. L., Costanzo, M., Boone, C., and Warren, A. J. (2007) *Nat. Genet.* **39,** 486–495
55. Granato, D. C., Gonzales, F. A., Luz, J. S., Cassiola, F., Machado-Santelli, G. M., and Oliveira, C. C. (2005) *FEBS J.* **272,** 4450–4463